

Doping Effects on the Charge-Density-Wave Dynamics in Blue Bronze

S. Yue¹, C. A. Kuntscher^{1a}, M. Dressel¹, S. van Smaalen², F. Ritter³, and W. Assmus³

¹ 1. Physikalisches Institut, Universität Stuttgart, Pfaffenwaldring 57, D-70550 Stuttgart, Germany

² Lehrstuhl für Kristallographie, Universität Bayreuth, 95440 Bayreuth, Germany

³ Physikalisches Institut, Universität Frankfurt, 60054 Frankfurt, Germany

Received: November 13, 2018

Abstract. The temperature dependences of the dc resistivity and the nonlinear transport properties in pure, Rb-doped, and W-doped blue bronze $K_{0.3}MoO_3$ single crystals are presented. In comparison with the Rb doping, the W doping has larger effects on the electrical transport properties and the Peierls transition. In particular, the maximum in the temperature dependence of the threshold field for nonlinear transport, observed in pure and Rb-doped samples around 100 K, is absent in W-doped $K_{0.3}MoO_3$. These results are discussed with respect to the proposed incommensurate-commensurate transition of the charge-density-wave and its interaction with impurities and normal carriers.

PACS. 71.45.Lr Charge-density-wave systems – 71.30.+h Metal-insulator transition and other electronic transitions

1 Introduction

Charge-density-waves (CDW) in low-dimensional solids attract interest since R. Peierls introduced this broken-symmetry ground state half a century ago [1]. Their dynamics has been subject to numerous investigations as soon as the first experimental realization became possible in the 1970s. The present state of knowledge is compiled in several reviews [2, 3, 4, 5, 6, 7]. Below the Peierls transitions, an energy gap opens at the Fermi energy leading to an insulating ground state. In the CDW phase the electronic transport has contributions from the normal charge carriers excited across the gap (like a semiconductor) and from the collective response of the CDW condensate. Although there exist a general idea about the main phenomena, a large number of observations are still puzzling and the details are not understood in depth. One of the key issues of the CDW dynamics is the interaction of the condensate with the underlying lattice and in particular with lattice imperfections.

Molybdenum bronze $A_{0.3}MoO_3$, where $A = K, Rb$ or Tl , is among the most-extensively studied quasi-one-dimensional compounds, which develops a CDW along the b axis below approximately 180 K [5]. In contrast to ideal systems the CDW condensate cannot move freely, but is pinned to the lattice by impurities and defects. This is easily seen, for instance, if an electric field is applied along the chain direction exceeding a critical value, the so-called first threshold field E_T ; as a consequence the

CDW is depinned, it begins to slide through the crystal and contributes additionally to the conductivity, resulting in a nonlinear current-voltage ($I - V$) response [8]. Below approximately $T = 40$ K for $K_{0.3}MoO_3$ a more complicated $I - V$ response is observed, including a second threshold field E_T^* above which a sharp increase of the current by many orders of magnitude occurs [9, 10, 11]. The temperature dependence of the first threshold field E_T is commonly explained by a sort of two-fluid model containing the electrons condensed in the CDW and the remaining normal electrons [12]; the approach describes the Coulomb interaction between the CDW and uncondensed charge carriers thermally excited above the Peierls gap. Within this model, with rising temperature the uncondensed carrier density increases, leading to an increasing damping of the CDW by dissipative normal currents and thus to an increase of E_T . However, when the temperature rises above $T = 100$ K a decrease of E_T is observed, resulting in a maximum of threshold field $E_T(T)$ around this temperature [8]. Similar observations were reported for the CDW compound TaS_3 [13]. The change in the temperature dependence of $E_T(T)$ might be attributed to an incommensurate-commensurate (I-C) transition of the CDW which happens around $T = 100$ K for blue bronze. However, small deviations from complete commensurability were found down to 4 K [14, 15, 16, 17] which somehow disturbs this picture. Interestingly, in comparison with $K_{0.3}MoO_3$ and TaS_3 , for $NbSe_3$ with two CDWs, which are always incommensurate with the underlying lattice, a very different temperature dependence of $E_T(T)$ was found [18]: The threshold field diverges at the Peierls tran-

^a email: kuntscher@pi1.physik.uni-stuttgart.de

sition temperature T_P and exhibits a minimum slightly below T_P . This behavior could be well described by the Fukuyama-Lee-Rice model for impurity pinning of the CDW [19,20] taking into account thermal fluctuations of the CDW phase [21]. For $\text{K}_{0.3}\text{MoO}_3$ different groups observed the maximum in $E_T(T)$ near $T = 100$ K, but its origin remains a puzzle.

The peculiarities of the CDW motion may be clarified by studying the doping dependence of $E_T(T)$. In blue bronze two types of substitution are possible, namely replacing K by isoelectronic Rb and the substitution of Mo by isoelectronic W. The two doping channels have a very different effect on the transport properties [22,23]. In blue bronze the oxygen octahedrons with the transition metal in the center form conducting chains along which the CDW develops. Obviously W substitution strongly disturbs the one-dimensional conduction and the development of the CDW, hence already a very small W concentration causes a large shift of the Peierls transition to lower temperature and a considerable broadening of the phase transition. For this so-called *strong* pinning the phase of the CDW is adjusted at each impurity site [19]. In contrast, the Rb dopants occupying the K sublattice only cause some disorder in the crystal potential and thus only play a minor role in the pinning mechanism; it is called weak pinning [19]. Measurements of $E_T(T)$ of $\text{K}_{0.3}\text{MoO}_3$ with 50% Rb doping for temperatures below 80 K show a similar behavior as in the pure compound [24]. However, the temperature dependence of the first threshold field for other Rb doping levels, and in particular for W-doped blue bronze compounds has not been measured up to now. Here we present a comprehensive study of $E_T(T)$ for a series of Rb- as well as of W-doped blue bronze compounds and discuss the origin of the maximum threshold observed around $T = 100$ K.

2 Experiments and Results

Pure, Rb-doped, and W-doped blue bronze $\text{K}_{0.3}\text{MoO}_3$ single crystals (see Table 1) were prepared by the temperature gradient flux method [25] and electrolytic reduction of the molten salts of $\text{A}_2\text{CO}_3\text{-MoO}_3$ for pure blue bronze $\text{A}_{0.3}\text{MoO}_3$ ($A=\text{K}$ and Rb), $\text{K}_2\text{CO}_3\text{-Rb}_2\text{CO}_3\text{-MoO}_3$ for Rb-doped $\text{K}_{0.3}\text{MoO}_3$, and $\text{K}_2\text{CO}_3\text{-MoO}_3\text{-WO}_3$ for W-doped $\text{K}_{0.3}\text{MoO}_3$. Different concentrations of the dopants in the melt determine the doping levels in the obtained crystals. For Rb-doped samples, the doping ratio is almost the same as that in the melt, but for the W-doped compounds, the doping ratio is nearly 2 to 3 times bigger than that in the melt [23,26]. The obtained samples have a typical size of $4\times 4\times 0.5$ mm³. In our dc electrical transport measurements a four-probe configuration was used. Thin gold wires were anchored by silver paint. In the contact regions, indium films were covered by gold films for stable contacting at low temperature. In this way, a typical contact resistance of around 1 Ω was achieved. For samples with the same doping level but grown by different preparation methods we obtained similar results.

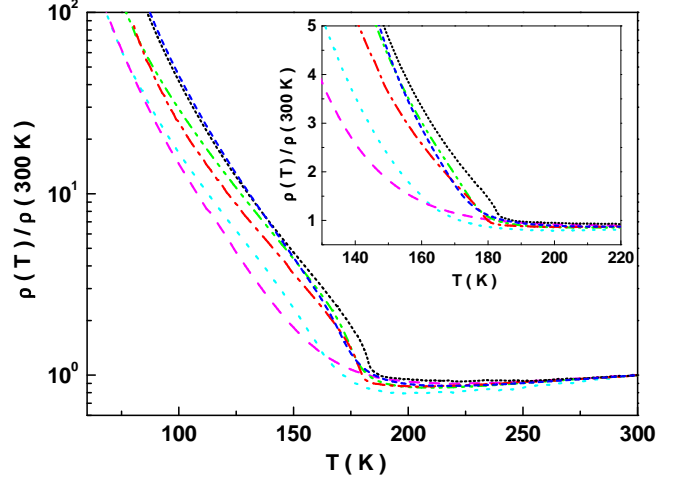


Fig. 1. Dc resistivity along the b axis, normalized to the room temperature value, for $\text{Rb}_{0.3}\text{MoO}_3$ (black short dot), $(\text{K}_{0.5}\text{Rb}_{0.5})_{0.3}\text{MoO}_3$ (blue short dash), $(\text{K}_{0.833}\text{Rb}_{0.167})_{0.3}\text{MoO}_3$ (green dash dot dot), $\text{K}_{0.3}\text{MoO}_3$ (red dash dot), $\text{K}_{0.3}\text{Mo}_{0.995}\text{W}_{0.005}\text{O}_3$ (cyan dot) and $\text{K}_{0.3}\text{Mo}_{0.99}\text{W}_{0.01}\text{O}_3$ (purple dash). The inset shows the enlargement of the results near the Peierls transition temperature T_P .

Fig. 1 shows the temperature dependence of the dc resistivity along the chain direction b normalized to the room temperature value for a series of pure and doped blue bronze crystals. The pure samples $\text{K}_{0.3}\text{MoO}_3$ and $\text{Rb}_{0.3}\text{MoO}_3$ show a sharp metal-semiconductor transition at the Peierls transition temperature T_P . The mixed compounds with 16.7% and 50% substitution of K by Rb still exhibit a clear transition T_P which is slightly shifted to lower temperatures. In contrast, for samples with small W doping (0.5%, 1%, and 2%, whose results are very similar to those of 1% doping and therefore not shown), the phase transition is significantly broadened. These results are consistent with previous reports [22].

To determine the Peierls transition temperature more precisely, we plot the derivative $D(T) = -\partial \ln \sigma / \partial T^{-1}$ versus temperature in Fig. 2. Except for the samples with 1% and 2% (not shown) W doping, all curves clearly show a peak around T_P ; the width ΔT_P is a measure of the sharpness of the transition [27]. Both the Rb and the W

Table 1. List of the studied blue bronze samples with the Peierls transition temperature T_P and the width of the transition ΔT_P [full width at half maximum of the derivative $D(T)$].

Sample	T_P (K)	ΔT_P (K)
$\text{Rb}_{0.3}\text{MoO}_3$	180.5	7.3
$(\text{K}_{0.5}\text{Rb}_{0.5})_{0.3}\text{MoO}_3$	170.7	36.3
$(\text{K}_{0.833}\text{Rb}_{0.167})_{0.3}\text{MoO}_3$	175.1	18.5
$\text{K}_{0.3}\text{MoO}_3$	179.2	11.2
$\text{K}_{0.3}\text{Mo}_{0.995}\text{W}_{0.005}\text{O}_3$	160.7	> 50
$\text{K}_{0.3}\text{Mo}_{0.99}\text{W}_{0.01}\text{O}_3$	≈ 140	—
$\text{K}_{0.3}\text{Mo}_{0.98}\text{W}_{0.02}\text{O}_3$	≈ 140	—

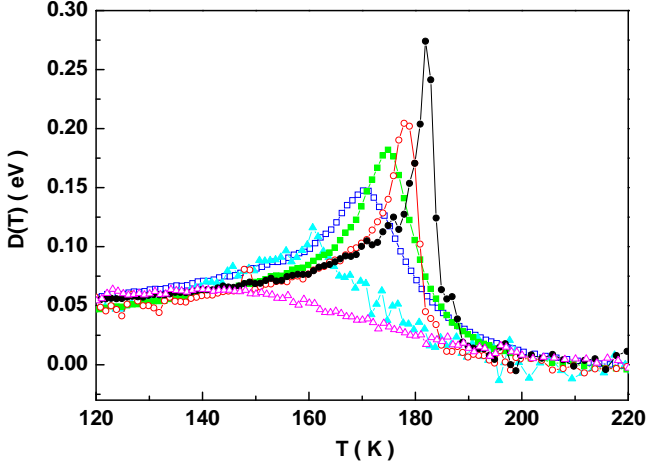


Fig. 2. The derivative $D = -\partial \ln \sigma / \partial T^{-1}$ versus temperature for $\text{Rb}_{0.3}\text{MoO}_3$ (black full circles), $\text{K}_{0.3}\text{MoO}_3$ (open red circles), $(\text{K}_{0.833}\text{Rb}_{0.167})_{0.3}\text{MoO}_3$ (full green squares), $(\text{K}_{0.5}\text{Rb}_{0.5})_{0.3}\text{MoO}_3$ (open blue squares), $\text{K}_{0.3}\text{Mo}_{0.995}\text{W}_{0.005}\text{O}_3$ (full cyan triangles), and $\text{K}_{0.3}\text{Mo}_{0.99}\text{W}_{0.01}\text{O}_3$ (open purple triangles).

doping lead to a shift of the transition to lower temperature and a broadening of the transition (see Table 1); however, these effects are considerably bigger in the case of W substitution.

We also studied the dc conductivity of pure and doped blue bronze single crystals along the chain direction b as a function of the applied electrical field. Two examples are displayed in Fig. 3. For temperatures below T_p the conductivity increases rapidly when the applied electric field exceeds the threshold field E_T due to the depinning of the CDW. The values of E_T were determined graphically from the $I - V$ characteristics. Fig. 4 summarizes the temperature dependences of the threshold field for blue bronze samples with different substitutions as indicated.

3 Discussion

The main results of our experiments can be summarized as follows: (i) Starting from the Peierls transition at $T_P = 180$ K, for pure $\text{K}_{0.3}\text{MoO}_3$ and $\text{Rb}_{0.3}\text{MoO}_3$ compounds E_T first increases upon cooling and then starts to decrease, resulting in a maximum in the behavior of $E_T(T)$ around $T = 100$ K; this agrees with previous data [8]. (ii) The substitution of K by Rb and of Mo by W does not influence the absolute value of E_T significantly; in fact, for temperatures above ≈ 50 K the E_T values for the W-doped samples are even slightly smaller than those for the pure samples, as found previously [24]. It is known that the absolute value of E_T depends on the properties of the sample, such as impurity concentration, cross section, and current distribution. (iii) For all the Rb-doped samples the threshold field $E_T(T)$ goes through a maximum value around $T = 100$ K when the temperature is lowered, like for the pure compound. However, even for very small W substitution on the Mo sites, the temperature dependence of

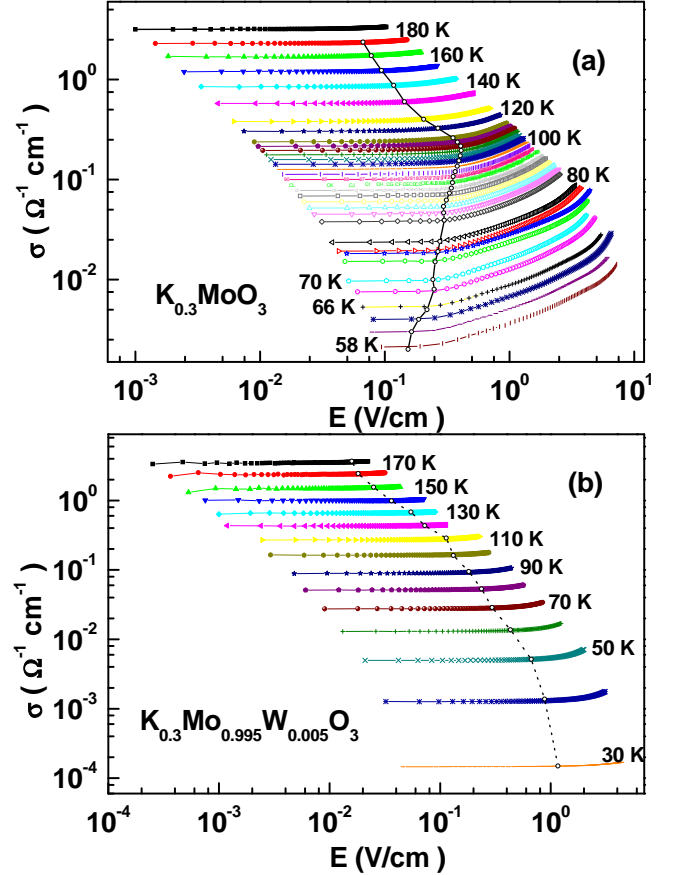


Fig. 3. Dc conductivity along the b axis as a function of applied electric field for several temperatures below the Peierls transition temperature T_p for (a) $\text{K}_{0.3}\text{MoO}_3$ and (b) $\text{K}_{0.3}\text{Mo}_{0.995}\text{W}_{0.005}\text{O}_3$. The dashed lines are guides to the eye for the variation of the threshold field with temperature.

the threshold field changed completely: $E_T(T)$ increases monotonously with decreasing temperature, and no maximum is observed within our experimental temperature range.

The non-monotonous temperature behavior of $E_T(T)$ observed for the CDW phase in blue bronze is puzzling. The most common explanation is the I-C transition of the CDW around $T = 100$ K. However, several observations contradict this hypothesis: If the CDW becomes commensurate with the underlying lattice for temperatures below $T = 100$ K, it should be strongly pinned and thus $E_T(T)$ is expected to increase below $T = 100$ K, in contrast to the experimental findings. Furthermore, substituting Mo by W adds pinning centers, but does not change the CDW nesting vector and its temperature dependence [14]; nevertheless for W-doped compounds the maximum in $E_T(T)$ is absent.

Certainly, there is no abrupt transition from an incommensurate to a commensurate CDW, but a continuous adjustment of the CDW to the underlying lattice; maybe this process saturates around $T = 100$ K [14]. It is known that down to $T = 4$ K small deviations from perfect commensuration remain [15, 16, 17]. Results from elec-

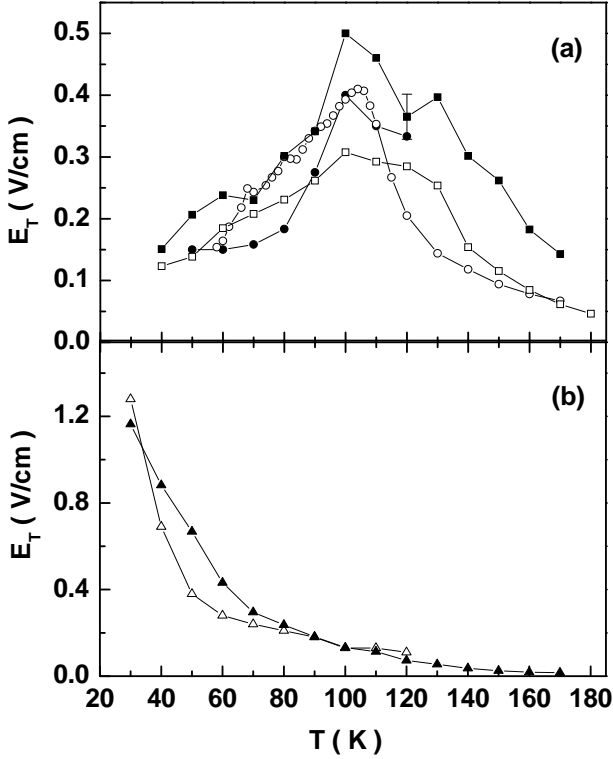


Fig. 4. Temperature dependence of the threshold field E_T along the b axis for (a) $\text{Rb}_{0.3}\text{MoO}_3$ (full circles), $\text{K}_{0.3}\text{MoO}_3$ (open circles), $(\text{K}_{0.833}\text{Rb}_{0.167})_{0.3}\text{MoO}_3$ (full squares), and $(\text{K}_{0.5}\text{Rb}_{0.5})_{0.3}\text{MoO}_3$ (open squares), and for (b) $\text{K}_{0.3}\text{Mo}_{0.995}\text{W}_{0.005}\text{O}_3$ (full triangles) and $\text{K}_{0.3}\text{Mo}_{0.99}\text{W}_{0.01}\text{O}_3$ (open triangles).

tron spin resonance experiments indicate the spatial coexistence of commensurate and incommensurate regions; when lowering the temperature from $T = 53$ K to 25 K the commensurate fraction increases from 5% to a value above 20% [17]. It was proposed [28] that even the incommensurate CDW consists of regions which are essentially commensurate with the lattice separated by discommensurations; these latter are narrow regions where the phase or displacement changes rapidly. At low temperature the CDW will then not move as a rigid object but propagate by depinned discommensurations, like the motion of grain boundaries and dislocations in the case of plastic deformation.

There are different effects relevant for the CDW transport, which might also influence the temperature dependence of the threshold field: (i) The CDW can interact with the underlying lattice in very different ways. Since for a commensurate CDW the interaction with the lattice is strong, mainly incommensurate domains of the CDW contribute to the collective transport. (ii) The CDW is not rigid, but subject to internal deformations, leading to a non-zero threshold field for nonlinear transport. These dynamic deformations of the CDW and dissipative normal currents need to be taken into account in order to explain $E_T(T)$. (iii) The interaction of the CDW with impurities or disorder either leads to strong or weak pinning

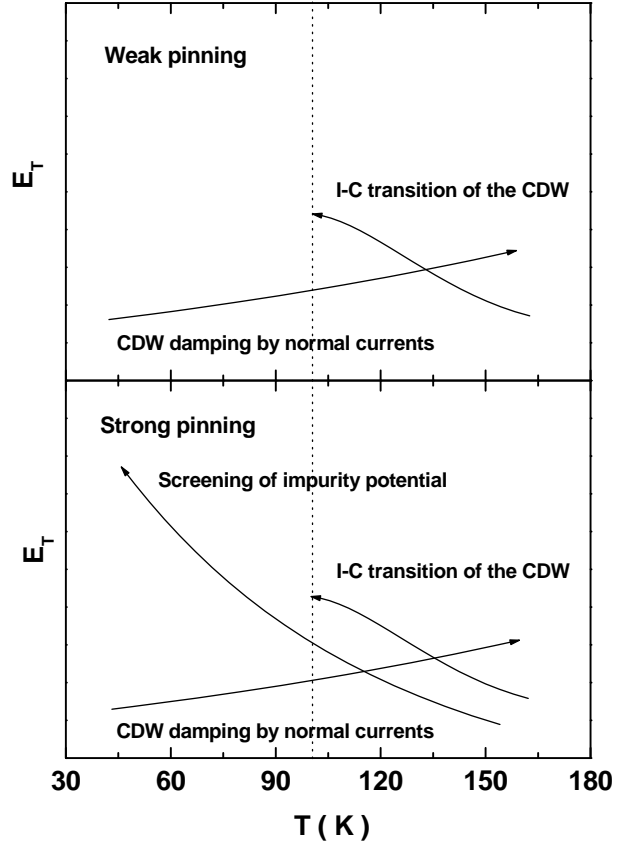


Fig. 5. Scheme of the various mechanisms relevant for the temperature dependence of the threshold field, $E_T(T)$, for weak pinning (top) and strong pinning (bottom).

of the CDW [19]. For strong pinning the CDW distorts its phase and amplitude locally at each impurity site; the CDW coherence length is therefore only on the order of the impurity spacing. In the case of weak pinning, the CDW adjusts its overall phase distribution within its coherence length, which is much larger than the impurity spacing. While the substitution of K by Rb pins the CDW only weakly, W doping causes strong pinning of the CDW [22].

The last two mechanisms will be strongly influenced by uncondensed electrons. According to Sneddon's model [12] the presence of uncondensed charge carriers will cause a damping of the CDW mode, since dissipative normal currents are induced by the dynamic deformations of the CDW. This is in agreement with previous investigations of the nonlinear characteristics of pure blue bronze, where a strong influence of the single-particle conductivity on the collective CDW response had been found [29]. Within this picture $E_T(T)$ increases with rising temperature, as the fraction of uncondensed carriers increases. Also the strength of the interaction of the CDW with lattice imperfections, like impurities or disorder, is influenced by the presence of normal charge carriers. This is in particular important in the case of strong pinning, since uncondensed carriers smoothen the CDW phase deformation induced by the strong pinning centers.

The temperature dependence of the threshold field E_T is determined by the above mentioned mechanisms, as illustrated in Fig. 5. In the course of the I-C transition the CDW becomes less discommensurate with decreasing temperature (with some sort of saturation around 100 K), which causes $E_T(T)$ to increase. According to Sneddon's two-fluid approach, the CDW damping by normal currents becomes less important as the temperature is reduced, leading to a decrease of $E_T(T)$. On the other hand, the screening of the impurity potential by uncondensed carriers will also depend on their density and thus on temperature, causing an increase of $E_T(T)$ as the temperature is lowered. This effect is expected to be only relevant for strong pinning, i.e., for W doping in the case of blue bronze, but not for weak pinning, i.e., Rb doping. This could explain why the maximum of $E_T(T)$ around $T = 100$ K is observed only for the Rb-doped compounds, but not for W-doped samples. For the latter compounds a smooth increase of $E_T(T)$ with decreasing temperature is found.

4 Conclusion

In order to investigate the influence of strong and weak pinning on the characteristics of the Peierls transition and on the first threshold field of non-linear conductivity, we studied the electrical transport properties of a series of pure, Rb-doped, and W-doped blue bronze $K_{0.3}MoO_3$ single crystals. For pure $K_{0.3}MoO_3$ crystals and for substitution of K by Rb, which acts as weak pinning center, the threshold field $E_T(T)$ exhibits a maximum around $T = 100$ K which is correlated with the incommensurate-to-commensurate transition of the CDW. A more advanced explanation requires to take into account the influence of the uncondensed charge carriers on the CDW transport.

5 Acknowledgements

The authors would like to thank Kazumi Maki, Attila Virosztek, and Silvia Tomic for helpful discussion and G. Untereiner for technical support. Financial support by the Deutsche Forschungsgemeinschaft (SPP 1073) is acknowledged.

References

1. R. E. Peierls, *Quantum theory of solids* (Clarendon, Oxford, 1955).
2. *Electronic Properties of Inorganic Quasi-one-dimensional Compounds*, Vol. I and II, edited by P. Monceau (Reidel, Dordrecht, 1985).
3. G. Grüner and A. Zettl, *Phys. Rep.* **119**, 117 (1985).
4. G. Grüner, *Rev. Mod. Phys.* **60**, 1129 (1988).
5. *Low-dimensional Electronic Properties of Molybdenum Bronzes and Oxides*, edited by C. Schlenker (Kluwer Academic Publishers, Dordrecht, 1989).
6. *Charge Density Waves in Solids*, edited by L.P. Gor'kov and G. Grüner, (North-Holland, Amsterdam, 1989).
7. G. Grüner, *Density Waves in Solids* (Addison-Wesley, Reading, MA, 1994).
8. J. Dumas, C. Schlenker, J. Marcus, and R. Buder, *Phys. Rev. Lett.* **50**, 757 (1983).
9. G. Mihaly and P. Beauchene, *Solid State Commun.* **63**, 911 (1987).
10. P. B. Littlewood, *Solid State Commun.* **65**, 1347 (1988).
11. S. Martin, R. M. Fleming, and L. F. Schneemeyer, *Phys. Rev. B* **38**, 5733 (1988).
12. L. Sneddon, *Phys. Rev. B* **29**, 719 (1984).
13. R. M. Fleming, R. J. Cava, L. F. Schneemeyer, E. A. Rietman, and G. Dunn, *Phys. Rev. B* **33**, 5450 (1986).
14. R. M. Fleming, L. F. Schneemeyer, and D. E. Moncton, *Phys. Rev. B* **31**, 899 (1985).
15. M. Sato, H. Fujishita, and S. Hoshino, *J. Phys. C* **16**, L877 (1983).
16. J. Pouget, C. Escribe-Filippini, B. Hennion, R. Currat, A.H. Moudden, R. Moret, J. Marcus, and C. Schlenker, *Mol. Cryst. Liq. Cryst.* **121**, 111 (1985).
17. A. Janossy, G.L. Dunifer, and J. S. Payson, *Phys. Rev. B* **38**, 1577 (1988).
18. R. M. Fleming, *Phys. Rev. B* **22**, 5606 (1980).
19. P. A. Lee and T. M. Rice, *Phys. Rev. B* **19**, 3970 (1979).
20. H. Fukuyama and P. A. Lee, *Phys. Rev. B* **17**, 535 (1978).
21. K. Maki and A. Virosztek, *Phys. Rev. B* **39**, 9640 (1989).
22. L. F. Schneemeyer, F. J. DiSalvo, S.E. Spengler, and J.V. Waszczak, *Phys. Rev. B* **30**, 4297 (1984).
23. L. G. Schneemeyer, R. M. Fleming, and S. E. Spengler, *Solid State Commun.* **53**, 505 (1985).
24. R. J. Cava, L. F. Schneemeyer, R. M. Fleming, P. B. Littlewood, and E. A. Rietman, *Phys. Rev. B* **32**, 4088 (1985).
25. K. V. Ramanujachary, M. Greenblatt, and W. H. McCarrroll, *J. of Crystal Growth* **70**, 476, 1984.
26. T. Mingliang, M. Zhiqiang, S. Jing, and Z. Yuheng, *Phys. Rev. B* **55**, 2107 (1997).
27. K. Carneiro, *Electronic Properties of Inorganic Quasi-one-dimensional Compounds*, edited by P. Monceau (Dordrecht, Reidel 1985), p. 44.
28. W. L. McMillan, *Phys. Rev. B* **14**, 1496 (1976).
29. G. Mihaly, P. Beauchene, J. Marcus, J. Dumas, and C. Schlenker, *Phys. Rev. B* **37**, 1047 (1988).